Journal of Medical Devices Technology
jmeditec.utm.my

Original Research

The Effect of Pore Length on the Mechanical Properties of Vascular Scaffold Due to Systolic Pressure

Nur Eszaty Farain Esa[1], Nurul Atiqah Maaruf [1], Musfirah Jiyanah Jahir-Hussain[1], and Norhana Jusoh[1, 2]

[1] School of Biomedical Engineering and Health Sciences, Faculty of Engineering, Universiti Teknologi Malaysia, 81310 Johor Bahru, Malaysia.
[2] Medical Devices and Technology Centre (MEDITEC), Institute of Human Centered Engineering, Universiti Teknologi Malaysia, 81310 Johor Bahru, Malaysia

ARTICLE INFO

Article History:
Received 19 November 2023
Accepted 16 December 2023
Available online 30 December 2023

Keywords:
3D-printing,
Vascular scaffold,
Systolic pressure,
Compression,
Tensile

ABSTRACT

Tissue replacements are highly limited due to the lack of vascularized tissue in the engineered tissue. Thus, incorporating the vascular scaffold in any injured tissue or organ is critical in the tissue regeneration. As one of elastic tissue in human body, mechanical properties are vital in engineering a vascular scaffold. Besides, interconnected pores and scaffold porosity are among the main considerations in designing the scaffold for allowing the vascularization. Therefore, this study aims to simulate the mechanical properties of three-dimensional (3D) printed vascular scaffold by observing the deformation and elasticity after being applied with the maximum systolic pressure. Scaffolds with three different pore lengths were simulated for compression and tensile analysis by using Finite Element Analysis (FEA) based on polyethylene terephthalate (PET) material's properties. The findings indicated that effective elastic modulus of the vascular scaffolds varied based on the pore length with shortest pore length gave the highest elasticity, whilst scaffold with the longest pore length gave lowest elasticity. Besides, stress value of compression and tensile analysis for all scaffolds were did not exceed the PET's yield strength that indicated the designed scaffolds will have high potential for vascular tissue engineering applications.

INTRODUCTION

Recently, the development of vascular networks culture models in vitro become rampant due to study of cellular and molecular aspects of angiogenesis, vasculogenesis and prevascularization of engineered tissues (Blache et al., 2018). For therapy, tissue vasculature design must be highly vascularized or able to promote the formation of new vasculatures at the vascular replacement site (Blache et. al., 2018). Besides good biocompatibility properties, tissue-engineered blood vessels should be able to withstand physiological pressures without aneurysm formation or leakage (Chang and Niklason, 2017). Hence, other issues related to current autografts and allografts are the lack control over physical and mechanical properties, inflammation, and calcification (Haasan et. al., 2014). In addition, the mechanical response of the arterial wall depends on the mechanical function of its passive components, the fibers of elastin and collagen, and the active component of the cells (Montini-Ballarin et. al., 2016). The mechanical properties of the vessel are evaluated by these components and each component contribution to the final elastic response can be defined (Montini-Ballarin et. al., 2016). In the study of human coronary artery scaffolding, mechanical properties that imitate native tissue in each layer are achieved by mimicking fiber angles and tuning vessel thickness, enabling close resemblance to the deformation profile and adherence of the human coronary artery itself (Akentjew et. al., 2019). An ideal functional tissue vascular line with the desired mechanical and biological characteristics that requires complete degradation with cell configuration and tissue remodelling (Thottappillil and Nair, 2015). The scaffold mechanical and biological durability is determined by the involvement of fibers and cells throughout the

* Norhana Jusoh (norhana@utm.my)

Medical Devices and Technology Centre (MEDITEC), Institute of Human Centered Engineering, Universiti Teknologi Malaysia, 81310 Johor Bahru, Malaysia

length and thickness of the graft (Akentjew et. al., 2019). Mechanical properties that are important for maintaining the stability of biomaterials are often compromised as a result of increased porosity. Better mechanical properties are important in the manufacture of vascular scaffolds, in order to provide sufficient support, particularly because of deterioration and loss of strength in wet conditions. Another important factor is the capacity of the scaffold itself, even though the structural and mechanical characteristics of the native vessels are expected to be progressively acquired through remodeling, repair, and post-implant development.

Moreover, polymers are vital for vascular application due to flexibility in the chemical, mechanical and biological properties of polymeric materials (Wenger and Giraud, 2018). However, the used of synthetic polymer like polylactic acid (PLA) in curing vascular disease also has restriction such as poor cell-recognition signals (Kao et. al., 2015). Nevertheless, polyethylene terephthalate (PET) has been used for fabricating and manufacturing the large diameter vascular prostheses and has demonstrated impressive mechanical strength and biocompatibility. A new paradigm in designing three-dimensional (3D) porous tissue engineering scaffolds is focused on the effect of scaffold parameters such as fiber size, porosity, number of cells per surface, number of layers and material selection in tuning the stiffness. As an example, the increasing of fiber length resulted on the increasing of the matrix stiffness, while the increasing of porosity contributed to the decreasing of the matrix stiffness (Vijayavenkataraman et. al., 2017). Fabrication technique like electrospinning often have relatively small pores and low in porosity, in which can inhibit cell infiltration into scaffolds that can prevent the cell development and growths which hindering the regeneration and remodelling of the vascular grafts (Tan et. al., 2016). 3D printing has emerged as one of the modern techniques for tissue engineering that could potentially produce scaffolds with or without cells that are useful in the treatment of cardiovascular diseases. This technique has attracted a great deal of attention due to its ability to treat diseases in tissue engineering and organ regeneration including the fabrication of the complex multicellular tissue (Liu et. al., 2017; Jammalamadaka and Tappa, 2018).

The development of porous scaffolds with high porosity materials allows the successful release of biofactors, such as proteins, genes, or cells, and provide good nutrient exchange substrates (Loh and Choong, 2013). Pore size has role in assessing the porosity of 3D scaffold. This is because cell processes can be influence by the changes in pore sizes. Interconnected pores of the outer porous surface have increase biocompatibility and enable more vascular ingrowth and incorporation (Vahidgolpayegani et. al., 2017). The role of pore size in tissue regeneration has been illustrated by studies that show an optimum pore size of 5 μm for neovascularisation (Murphy and O'Brien, 2010). The pore size needs to be large enough for the indirect contact of cell across the scaffold, to ensure cell nutrition but not too large to stop cell migration (Bružauskaitė et. al., 2016). This is because large pores will reduce the surface area that restricts cell adhesion. The ECM architecture offers courses for cellular contact facilitated by the interaction of integrins with ECM proteins (Vahidgolpayegani et. al., 2017). Therefore, the vascular tissue engineering development is depending on putting all things together in producing a highly engineered grafting with a robust off-the-shelf time and cost effectiveness (Li et. al., 2014). Therefore, this study aims to design 3D-printed vascular scaffold and to simulate the mechanical properties of the scaffold based on PET material in observing the deformation and elasticity of the PET's scaffold after being applied by the maximum systolic pressure presence in the larger arteries.

FINITE ELEMENT ANALYSIS

The geometries morphological shape of the scaffold was cylinder in which the scaffolds were designed layer by layer and crossing each other in every layer to make holes or pores in between the crossing area (Kao et. al., 2015; Laschke et. al., 2008). All the designs were fixed in radius (6 mm) and height (12 mm) with the bilateral tolerance of 0.5 mm as shown in Figure 1.

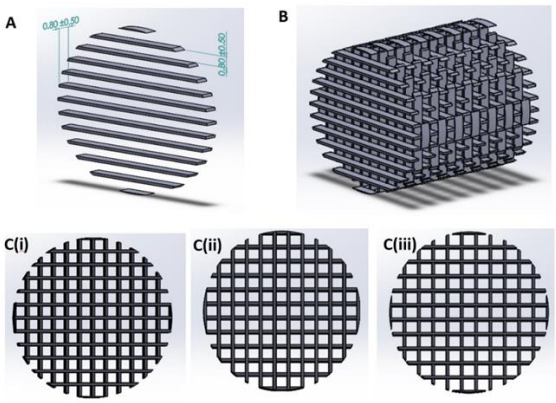

Fig 1 The structure of vascular scaffold with different pore size with A) dimension of a piece layer of the scaffold, (B) complete cylinder shape of the scaffold, C(i) design A with porous length of 0.80 mm, C(ii) design B with porous length of 0.85 mm and C(iii) design C with porous length of 0.90 mm.

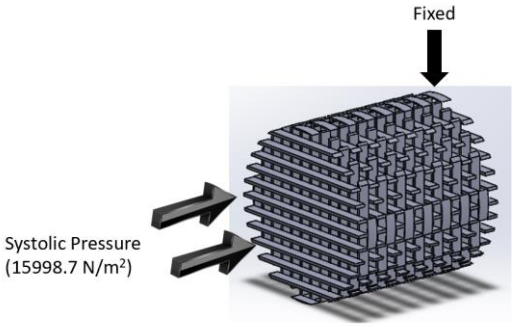

Fig 2 The direction of applied force and the fixed support.

A finite element analysis (FEA) was carried out to predict the compression and tensile properties using the SolidWorks software (Karuppudaiyan et. al., 2018). Two types of static analysis, uniaxial compression and tensile testing, were conducted to observe the mechanical behaviour of the PET material (Castillo-Cruz et al., 2018). PET has been chosen as a vascular scaffold material as it is a highly biocompatible material. PET is a stiff polymer known for fabricating large vascular prostheses (Khodadoust et., al., 2018; Samavedi et. al., 2014). Three types of static analysis were conducted for both uniaxial compression and tensile testing: stress, strain and displacement analysis. The systolic pressure of 15998.7 N/m2 was applied to the scaffolds to represent the pressure at the walls

of larger arteries. The direction of the applied force is in uniaxial direction, and the end of the scaffold is fixed, as shown in Figure 2.

RESULT AND DISCUSSION

Porosity plays an important role in designing vascular scaffolds. Interconnected pores within the scaffolds are vital for the transfer of nutrients and oxygen for cell vascularization and proliferation (Liu and Yan 2018). Therefore, all the designs also need to have a porosity within the range as it is also the main factor in designing vascular scaffold geometry. Table 1 shows the volumetric properties of the scaffold.

Table 1 Volumetric properties of the scaffold

Properties	Pore Length		
	A (0.80mm)	B(0.85mm)	C(0.90mm)
Porous length (mm)	0.80	0.85	0.90
Total volume (mm^3)	1357.17	1357.17	1357.17
Volume of solid (mm^3)	268.03	257.88	235.82
Volume of porous (mm^3)	1089.12	1099.29	1121.35
Porosity (%)	80.25	81.00	82.62

As shown in Table 1, the porosity of all designs was within optimal range for vascular scaffold, which were 80% to 90% (Hu et. al., 2010; Song et. al., 2011). Furthermore, scaffold with longest pore length (0.90 mm) has the highest porosity (82.62%). Thus, the porosity of each design depends on the pore length with longer pore length resulting in a higher porosity of the scaffold and vice versa. Figures 3 shows the stress, strain and displacement analysis for uniaxial compression testing by using PET's material properties.

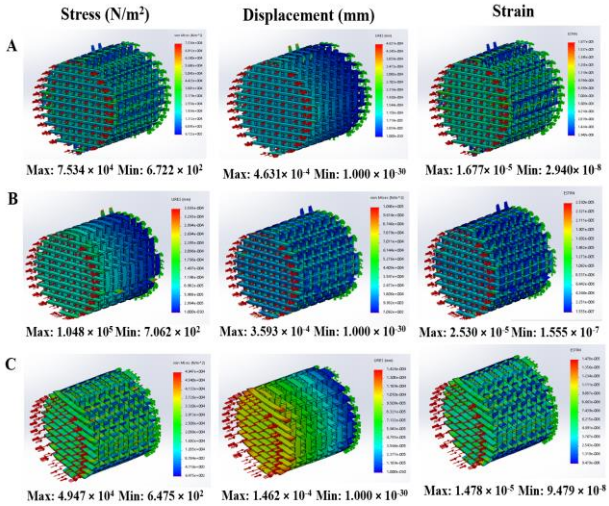

Fig 3 Von Mises stress contour plots due to compression testing of systolic pressure of 15998.7 Pa for scaffold with different pore length A) 0.80mm, B) 0.85mm and C) 0.90mm.

Figure 3 shows the results of stress, strain and displacement when the systolic pressure of 15998.7 Pa was applied to the solid body. From the result, the maximum stress for systolic pressure experienced by design A was $7.534x10^4$ N/m^2 while the minimum stress was $6.772x10^2$ N/m^2. Meanwhile, the maximum amount of von Mises stress for design B was $1.048x10^5$ N/m^2 and the minimum value was $7.062x10^2$ N/m^2. The maximum amount of von Mises stress experienced by design C after being applied by systolic pressure was $4.947x10^4$ N/m^2 and the minimum value of stress was $6.475x10^2$N/m^2. To conclude, stress analysis for all the three designs did not exceed the yield strength of PET material, which is $40x10^6$ N/m^2 (Samavedi et. al., 2014), that indicates the limit of elastic behaviour and the beginning of plastic behaviour. The displacement analysis shows that design A undergo maximum displacement of $4.631x10^{-4}$ mm and minimum displacement of $1.000x10^{-30}$ mm. Therefore, design A was considered safe to be used as a vascular scaffold due to low risk of deformation. Meanwhile design B experienced maximum displacement of $3.593x10^{-4}$ mm and minimum value of $1.000x10^{-30}$ mm. Design C has the maximum displacement of $1.462x10^{-4}$ mm and minimum displacement of $1.000x10^{-30}$ mm that shows a different colour contour on the geometry which indicates that the red colour part experienced the most displacement compared to the other parts. Based on this pressure data, design C was considered to perceive a slightly high deformation of the solid body compared to other designs.

Furthermore, strain analysis result for design A indicates that the maximum value of $1.677x10^{-5}$ and the minimum value of $2.940x10^{-8}$. The amount of maximum strain in the material indicated that the solid body does not undergo lot of dimensional changes when the pressure is being applied. Then, the strain analysis result for design B shows that the maximum value was $2.530x10^{-5}$ and the minimum value is $1.555x10^{-7}$. These data show that the maximum strain was not high and will not cause the PET material to shift or slip from its place. Moreover, strain analysis for design C shows the maximum value of $1.478x\ 10^{-5}$ and minimum value of $9.479x10^{-8}$. The amount of maximum strain of the design C suggested that the solid body did not undergo a lot of dimensional adjustments when the systolic pressures is applied. Figure 4 shows the stress, strain and displacement analysis for uniaxial tensile testing based on PET's material properties. The purpose of tensile test was to determine and pinpoint the onset of plastic deformation which is the yield point on the scaffold (Castillo-Cruz et. al., 2018).

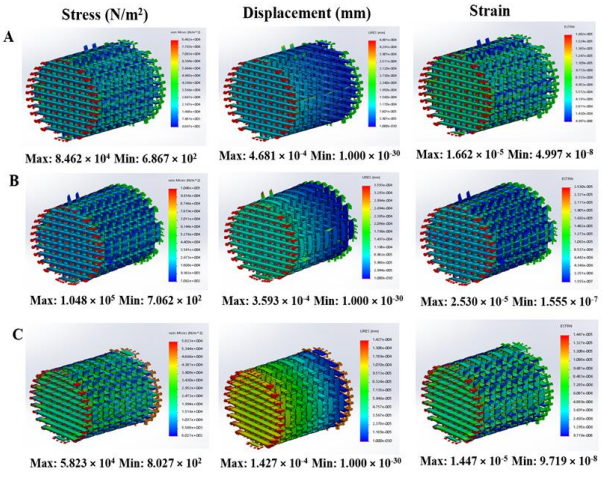

Fig 4 Von Mises stress contour plots due to tensile testing of systolic pressure of 15998.7 Pa for scaffold with different pore length A) 0.80mm, B) 0.85mm and C) 0.90mm.

As shown in Figure 4, the maximum amount of von Mises stress experienced by design A is $8.462x10^4$ N/m^2 and the minimum value was $6.867x10^2$ N/m^2. However, both values did not exceed the PET yield strength's value of $40x10^6$ N/m^2. Meanwhile, the systolic pressure applied on the design B gave a maximum amount of von Mises stress of 1.048×10^5 N/m^2 and the minimum value of $7.062x10^2$ N/m^2. Furthermore, the maximum

amount of von Mises stress experienced by design C was $5.823x10^4$ N/m^2 and the minimum value is $8.027x10^2$ N/m^2. However, both values did not exceed the PET yield strength which was $40x10^6$ N/m^2. Therefore, the maximum von Mises stress for all scaffold designs were below the yield strength that indicates the scaffolds were within the safe limit and will not cause any harmful issue to the patient.

Next, systolic pressure caused the maximum displacement of design A was $4.681x10^{-4}$ mm and minimum displacement value of $1.000x10^{-30}$ mm. For design B, the maximum value was $3.593x10^{-4}$ mm and minimum value was $1.000x10^{-30}$ mm for displacement. Based on data obtained, design A and B was considered safe to be used as a vascular scaffold due to the relatively low risk of deformation. For design C, the maximum displacement value was $1.427x10^{-4}$ mm and minimum displacement value of $1.000x10^{-30}$mm after being applied by systolic pressure. Design C also shows a different colour contour on the geometry which indicates that the red colour part experienced the most displacement compared to the other parts.

Furthermore, the strain analysis result for design A shows that the maximum value was $1.662x10^{-5}$ while the minimum value is $4.997x10^{-8}$. Both value of strain suggested that the solid body did not undergo a lot of dimensional adjustments when the pressure was applied. Meanwhile, for design B, the strain analysis shows that the maximum value was $2.530x10^{-6}$ and the minimum value was $1.555x10^{-7}$. This data shows that design B has lower strain which result to lower resistance of stress, thus, low mechanical strength. Then, the strain analysis result for design C shows that the maximum value was $1.447x10^{-5}$ and the minimum value was $9.719x10^{-8}$, that show the design C has lowest resistance to the stress and lowest strength compared to design A and design B.

These results show that pore length contributed to the mechanical properties improvement in term of ultimate tensile stress. Design B underwent higher stress distribution exerted on the geometry which resulted in high strain and high deformation of the geometry. However, all designs have low maximum tensile stress compared to the yield strength of PET material which indicate the limit of elastic behaviour and the beginning of plastic behaviour. The effective elastic modulus under systolic pressure for all scaffolds were predicted by using finite element modelling approach, as shown in Table 2.

Table 2 Mechanical properties of scaffolds under systolic pressure

	Porosity (%)	Compression Effective Elastic Modulus (GPa)	Tensile Effective Elastic Modulus (GPa)
A (0.80mm)	80.25	4.493	5.091
B (0.85mm)	81.00	4.142	4.142
C (0.90mm)	82.62	3.347	4.024

As shown in Table 2, Design A with lowest porosity has the highest effective elastic modulus of 4.493 GPa and 5.091 GPa, for compression and tensile tests, respectively. However, design B with moderate porosity has the intermediate effective elastic modulus of 4.412 GPa for both compression and tensile test. Design C with the highest porosity has the lowest effective elastic modulus of 3.347 GPa for compression test and 4.024 GPa for tensile test. These results show that the effective elastic modulus vary depends on geometry porosity. All designs have higher value of effective elastic modulus which is compatible as elastic vascular scaffold.

CONCLUSION

PET vascular scaffolds with different pore length were designed and were simulated for mechanical properties in predicting the effect of pore length on compression and tensile properties based on systolic pressure. The finding indicates that effective elastic modulus depends on the length of porous and porosity of the geometry. All three designs undergo elastic deformation, which scaffold with 0.90mm pore length was the most flexible design compared to other scaffolds. Scaffold with shortest pore length have the lowest scaffold porosity, but with the highest elasticity. Meanwhile, the scaffold with the longest pore length has higher porosity but with low elasticity. Therefore, we can conclude that design C(0.90mm) was the best design due to high porosity that critical for cell development and growth, and low elastic property that enable vascular scaffold to withstand the systolic pressure. These findings support the suitability of the PET vascular scaffold with define elastic properties which suitable for vascular replacement.

ACKNOWLEDGEMENT

The authors would like to acknowledge Universiti Teknologi Malaysia for funding through Research University Grant Scheme Tier 2 (Q.J130000.2651.17J03).

REFERENCES

Akentjew, T. L., Terraza, C., Suazo, C., Maksimcuka, J., Wilkens, C. A., Vargas, F., Zavala, G., Ocaña, M., Enrione, J., García-Herrera, C., Valenzuela, L. M., Blaker, J. J., Khoury, M., & Acevedo, J. P. 2019. Rapid fabrication of reinforced and cell-laden vascular grafts structurally inspired by human coronary arteries. Nature Communications, 10, 1-15.

Blache, U., Guerrero, J., Güven, S., Klar, A. S., & Scherberich, A. 2021. Microvascular networks and models: in vitro formation. Vascularization for Tissue Engineering and Regenerative Medicine, 345-383.

Bružauskaitė, I., Bironaitė, D., Bagdonas, E., & Bernotienė, E. 2015. Scaffolds and cells for tissue regeneration: different scaffold pore sizes—different cell effects. Cytotechnology, 68(3), 355–369.

Castillo-Cruz, O., Pérez-Aranda, C., Gamboa, F., Cauich-Rodríguez, J., Mantovani, D., & Avilés, F. 2018. Prediction of circumferential compliance and burst strength of polymeric vascular grafts. Journal of the Mechanical Behavior of Biomedical Materials, 79, 332–340.

Chang, W.G. and Niklason, L.E. 2017. A short discourse on vascular tissue engineering. NPJ Regen Med 2 (1). 1–8.

Hasan, A., Memić, A., Annabi, N., Hossain, M., Paul, A., Dokmeci, M. R., Dehghani, F., & Khademhosseini, A. 2014. Electrospun scaffolds for tissue engineering of vascular grafts. Acta Biomaterialia, 10(1), 11–25.

Hu, J., Sun, X., Ma, H., Xie, C., Chen, Y. E., & Peter, X. 2010. Porous nanofibrous PLLA scaffolds for vascular tissue engineering. Biomaterials, 31(31), 7971–7977.

Jammalamadaka, U., & Tappa, K. 2018. Recent advances in biomaterials for 3D printing and tissue engineering. Journal of Functional Biomaterials, 9(1), 22.

Kao, C. T., Lin, C., Chen, Y. W., Yeh, C. H., Fang, H. Y., & Shie, M. 2015. Poly(dopamine) coating of 3D printed poly(lactic acid) scaffolds for bone tissue engineering. Materials Science and Engineering: C, 56, 165–173.

Karuppudaiyan, S., Singh, D. K. J., & Santosh, V. M. 2018. Finite element analysis of scaffold for large defect in femur bone. IOP Conference Series, 402, 012096.

Khodadoust, M., Mohebbi-Kalhori, D., & Jirofti, N. 2018. Fabrication and characterization of electrospun bi-hybrid PU/PET scaffolds for small-diameter vascular grafts applications. Cardiovascular engineering and technology, 9(1), 73-83.

Laschke, M. W., Rücker, M., Jensen, G., Carvalho, C., Mülhaupt, R., Gellrich, N., & Menger, M. D. 2007. Incorporation of growth factor containing Matrigel promotes vascularization of porous PLGA scaffolds. Journal of Biomedical Materials Research Part A, 85A(2), 397–407.

Li, S., Sengupta, D., & Chien, S. 2013. Vascular tissue engineering: from in vitro to in situ. WIREs Mechanisms of Disease, 6(1), 61–76.

Liu, H., Zhou, H., Lan, H., Li, T., Liu, X., & Yu, H. 2017. 3D printing of Artificial blood vessel: Study on Multi-Parameter Optimization Design for Vascular Molding effect in alginate and gelatin. Micromachines, 8(8), 237.

Liu, J., & Yan, C. 2018. 3D printing of scaffolds for tissue engineering. 3D Printing, 1789239664. pp.137-154.

Loh, Q. L., & Choong, C. 2013. Three-Dimensional scaffolds for tissue engineering applications: role of porosity and pore size. Tissue Engineering Part B-reviews, 19(6), 485–502.

Montini-Ballarin, F., Calvo, D., Caracciolo, P. C., Rojo, F. J., Frontini, P. M., Abraham, G. A., & Guinea, G. V. 2016. Mechanical behavior of bilayered small-diameter nanofibrous structures as biomimetic vascular grafts. Journal of the Mechanical Behavior of Biomedical Materials, 60, 220–233.

Murphy, C. M., & O'Brien, F. J. 2010. Understanding the effect of mean pore size on cell activity in collagen-glycosaminoglycan scaffolds. Cell Adhesion & Migration, 4(3), 377–381.

Samavedi, S., Poindexter, L. K., Van Dyke, M., & Goldstein, A. S. 2014. Synthetic biomaterials for regenerative medicine applications. In Organ Transplantation edited by G. Orlando, J. Lerut, S. Soker, R. J. Stratta (Academic Press, 2014) pp. 81-99.

Song, Y., Feijén, J., Grijpma, D. W., & Poot, A. A. 2011. Tissue engineering of small-diameter vascular grafts: A literature review. Clinical Hemorheology and Microcirculation, 49(1–4), 357–374.

Tan, Z., Wang, H., Gao, X., Liu, T., & Tan, Y. 2016. Composite vascular grafts with high cell infiltration by co-electrospinning. Materials Science and Engineering: C, 67, 369–377.

Thottappillil, N. and Nair, P.D., 2015. Scaffolds in vascular regeneration: current status. Vascular health and risk management, pp.79-91.

Vahidgolpayegani, A., Wen, C., Hodgson, P., & Li, Y. 2017. Production methods and characterization of porous Mg and Mg alloys for biomedical applications. In Metallic Foam Bone, edited by Wen C. (Woodhead Publishing, 2017) pp 25-82.

Vijayavenkataraman, S., Zhang, S., Fuh, J. Y. H., & Lu, W. F. 2017. Design of Three-Dimensional Scaffolds with Tunable Matrix Stiffness for Directing Stem Cell Lineage Specification: An In Silico Study. Bioengineering, 4(4), 66.

Wenger, R., & Giraud, M. 2018. 3D printing applied to tissue engineered vascular grafts. Applied Sciences, 8(12), 2631.